J. Resour. Ecol. 2024 15(5): 1147-1159
DOI: 10.5814/j.issn.1674-764x.2024.05.004
www.jorae.cn

# Vegetation Changes from 2014 to 2023 in the Mongolian Plateau Permafrost Region under Climate Change

LI Fengjiao[1,2], WANG Juanle[2,3,4,*], LI Pengfei[1], Davaadorj DAVAASUREN[5]

1. College of Geomatics, Xi'an University of Science and Technology, Xi'an 710054, China;
2. State Key Laboratory of Resources and Environmental Information System, Institute of Geographic Sciences and Natural Resources Research, Chinese Academy of Sciences, Beijing 100101, China;
3. College of Resources and Environment, University of Chinese Academy of Sciences, Beijing 100049, China;
4. Jiangsu Center for Collaborative Innovation in Geographical Information Resource Development and Application, Nanjing 210023, China;
5. Department of Geography, School of the Art and Sciences, National University of Mongolia, Ulaanbaatar 14201, Mongolia

**Abstract:** The permafrost region is one of the most sensitive areas to climate change. With global warming, the Mongolian Plateau permafrost is rapidly degrading, and its vegetation ecosystem is seriously threatened. To address this challenge, it is essential to understand the impact of climate change on vegetation at different permafrost degradation stages on the Mongolian Plateau. Based on the general permafrost distribution, in this study，we divided different permafrost regions and explored the response of vegetation to climate change at different stages of permafrost degradation by the idea of "space instead of time" from 2014 to 2023. The results of the study showed that: (1) Normalized difference vegetation index (NDVI) values showed a decreasing trend, and the proportion of the decreasing region was in the order of sporadic permafrost region > isolated and sparse permafrost region > continuous and discontinuous permafrost regions. (2) The main controlling factors of vegetation growth in permafrost regions are different, air temperature is the main controlling factor of vegetation growth in isolated and sparse permafrost region ($r$=–0.736) and sporadic permafrost regions ($r$=–0.522), and precipitation is the main controlling factor of vegetation growth in continuous and discontinuous permafrost region ($r$=–0.498). (3) The response of NDVI to climate change varies at different stages of permafrost degradation. In the early stages of permafrost degradation, increased land surface temperature (LST) and air temperature favored vegetation growth and increased vegetation cover, whereas increased precipitation impeded vegetation growth; as the permafrost degraded, increased LST and air temperature impeded vegetation growth, whereas increased precipitation promoted vegetation growth.

**Key words:** Mongolian Plateau; MODIS; NDVI; permafrost; vegetation changes

## 1 Introduction

Permafrost is defined as land with temperatures equal to or below 0 ℃ for two or more consecutive years (Zhang et al., 2000; Short et al., 2011; Wang et al., 2018). It is distributed over a wide range of cold regions and is an important component of the cryosphere, Its response to global change is rapid and indicative (Gao, 2019). Climate change-induced degradation of permafrost reshapes or alters permafrost vegetation ecosystems by changing the environment in which

**Received:** 2024-01-12 **Accepted:** 2024-04-26
**Foundation:** The National Natural Science Foundation of China (32161143025); The Science & Technology Fundamental Resources Investigation Program of China (2022FY101905); The National Key R&D Program of China (2022YFE0119200); The Mongolian Foundation for Science and Technology (NSFC_2022/01, CHN2022/276); The Key R&D and Achievement Transformation Plan Project in Inner Mongolia Autonomous Region (2023KJHZ0027); The Key Project of Innovation LREIS (KPI006); The Construction Project of China Knowledge Center for Engineering Sciences and Technology (CKCEST-2023-1-5).
**First author:** LI Fengjiao, E-mail: lifj@lreis.ac.cn
***Corresponding author:** WANG Juanle, E-mail: wangjl@igsnrr.ac.cn

**Citation:** LI Fengjiao, WANG Juanle, LI Pengfei, et al. 2024. Vegetation Changes from 2014 to 2023 in the Mongolian Plateau Permafrost Region under Climate Change. *Journal of Resources and Ecology*, 15(5): 1147–1159.

the vegetation grows, resulting in changes in vegetation cover. For example, boreal forests have disappeared (Baltzer et al., 2014), and there have been changes in vegetation cover (Tutubalina and Rees, 2001), grassland vegetation composition and productivity (Schuur et al., 2007), biomass (Guo et al., 2017b), vegetation (Sun et al., 2014), net primary productivity (Mao et al., 2015), biodiversity (Beilman, 2001), and vegetation communities.

The permafrost region is one of the most sensitive areas to climate change, and its ecosystems, especially vegetation ecosystems, are highly susceptible to disturbances from external conditions. The Mongolian Plateau permafrost region is located between the high-altitude and high-latitude permafrost regions of the Northern Hemisphere and is capable of responding rapidly to global change (Gao, 2019; Ma et al., 2022). Permafrost degradation on the Mongolian Plateau is becoming increasingly severe and the rate of degradation is increasing. The rate of permafrost degradation on the Mongolian Plateau was $9.1\times10^3$ km$^2$ yr$^{-1}$ in 2003–2019 (Gao et al., 2022). This has led to a warming of the ground temperature in the region, which in turn has altered the active permafrost layer and hydrothermal state (Ma et al., 2022). The increased thickness of the active layer owing to the degradation of permafrost directly affects plant growth by altering moisture and soil temperature (Strozzi et al., 2018; Klinge et al., 2021). Consequently, this affects plant species richness and vegetation cover. Vegetation responds differently to permafrost degradation, depending on its stage and the condition of the growing environment. In areas with shallow thaw depths, permafrost degradation may increase soil moisture with a gradual expansion of aquatic or wet plants and an increase in vegetation cover (Jorgenson et al., 2001). However, with the gradual deepening of the active layer and improved drainage, the water table decreases, water in the vegetation rhizosphere decreases, the ground temperature increases, and the ground surface tends to be dryer. This may increase the number of arid and mesophytic plants, decrease the number of aquatic and wet plants and expand the area of bare ground. This decreases the extent and productivity of the vegetation cover (Wang et al., 2006; Chen et al., 2010; Chen et al., 2011; Chen et al., 2012).

Normalized difference vegetation index (NDVI) datasets, an effective remote sensing tool for monitoring vegetation growth, haves been widely applied in permafrost regions (Bhatt et al., 2013; Vrieling et al., 2013). Wang et al. (2016) analyzed the changing trend of alpine grassland on the Tibetan Plateau between 1982 and 2012 using the NDVI dataset. Guo et al. (2017a) analyzed the spatiotemporal variations in the growing-season NDVI in the permafrost region of northeastern China and the correlation between NDVI and ground surface temperatures from 1981 to 2014. However, research on the effects of permafrost degradation on vegetation is still insufficient, and in the absence of long-term monitoring, the "space instead of time" approach has been used to compare the nature of vegetation ecosystems under different permafrost conditions and hypothesized changes in vegetation ecosystems and permafrost conditions (Wang et al., 2012; Qin et al., 2013; Zhou et al., 2015; Guo et al., 2017b). To date, most of these studies have focused on the Tibetan Plateau and the permafrost region of northeastern China, with relatively few studies conducted on the permafrost region of the Mongolian Plateau. This is particularly true in the context of climate change, in which changes in vegetation cover have rarely been reported.

In this study, we analyzed the spatial distribution and trends of vegetation in the permafrost region of the Mongolian Plateau from 2014 to 2023 using NDVI data. To avoid anomalous NDVI values from winter snow cover, the average NDVI during the vegetation growing season (April–October) was used (Guo et al., 2017b; Guo et al., 2022). In addition, the effect of climate change on NDVI in different types of permafrost regions was analyzed by examining the correlation between NDVI trends and land surface temperature (LST), air temperature and precipitation trends. This study aimed to enhance our understanding of the direct and indirect impacts of permafrost degradation on Mongolian Plateau ecosystems and to provide a scientific basis for research on the responses of these permafrost ecosystems to climate warming.

## 2 Study area and research methods

### 2.1 Study area

The Mongolian Plateau is located in a transition zone between Siberian coniferous forests and desert steppes in Central Asia (Liu et al., 2009). It stretches from the Daxingan Mountains in the east to the Altai Mountains in the west, bounded to the north by the Sayan Ridge and the Yabronov Mountains, and to the south by the Yinshan Mountain Range. It encompasses the entirety of Mongolia; the Republics of Tuvar, Buryatia, and Transbaikal Krai in southern of Russia, and part of China's Inner Mongolia Autonomous Region and the Xinjiang Uygur Autonomous Region (Fig. 1).

In this study, a permafrost region within the Mongolian Plateau, with an area of approximately $1.90\times10^6$ km$^2$, located in the north-central part of the Mongolian Plateau, was selected as the study area. This area was selected from the National Cryosphere Desert Data Center's permafrost and permafrost zoning map of the Republic of Mongolia and the 1:2.5 million permafrost type dataset for Russia (Fig. 1). The study area has a temperate continental climate, with an average annual precipitation of approximately 200 mm. The climate is characterized by cold and long winters from November to April, with minimum temperatures down to −40 ℃, short springs from May to June, and autumns from September to October, which are often characterized by sudden weather events. The summer months from July to August, often have large diurnal temperatures, abundant light, and

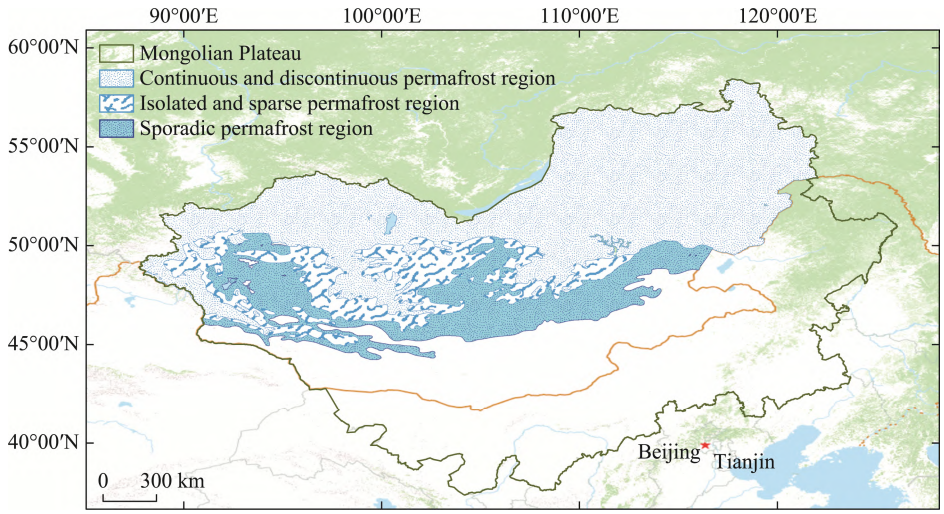


Fig. 1 Overview of the study area

strong ultraviolet rays, with maximum temperatures up to 35 ℃ (Zhou et al., 2012).

## 2.2 Data sources and data processing

### 2.2.1 Permafrost distribution data

Permafrost distribution data were downloaded from the "Map of Permafrost and Permafrost Zoning in the Republic of Mongolia", and the "Russian 1:2.5 Million Permafrost Type Dataset" from the National Cryosphere Desert Data Center (http://www.ncdc.ac.cn) (Sodnom and Yanshin, 1990; Li, 2019). These data were digitized from a map of the "Geocryology and Geocryological Zonation of Mongolia" derived from the "National Atlas of Mongolia" (Sodnom and Yanshin, 1990) and "Digitization of the Russian 1:2.5 Million Permafrost Type Dataset". From 1991 to 1996, Russia published a 1:2.5 million Geocryological Map of Russia and the Neighboring Republics series of 16 maps, which are labeled Russian. In 1998, Zaitsev et al. translated this scale into English (Li, 2019). In the study area, the permafrost distribution area of Mongolia was selected from the "Map of Permafrost and Permafrost Zoning in the Republic of Mongolia", and the remainder was selected from the "1:2.5 Million Permafrost Types Dataset of Russia". Seasonal and fragmented permafrost regions were deleted by cropping, merging, and deleting of elements using ArcMap 10.6. This was used to obtain a contiguous permafrost map of the Mongolian Plateau (Fig. 1). Here after, this region will be referred to as the Mongolian Plateau permafrost region. The study area was divided into continuous and discontinuous permafrost, with more than 50% of the ground surface in true permafrost, isolated and sparse permafrost with 10%–50% of the ground surface in true permafrost, and sporadic permafrost with less than 10% of the ground surface in true permafrost. Part of the permafrost region in northeastern China forms a part of the Mongolian Plateau. However, this area is relatively small and was not analyzed in the present study.

### 2.2.2 NDVI data

The NDVI data were derived from MOD13Q1 (h23v03, h23v04, h24v03, h24v04, h25v03, h25v04, h26v03, and h26v04) Terrestrial Level 3 standard data products provided by NASA from September 2013 to August 2023, with a spatial resolution of 250 m and a temporal resolution of 16 d. Downloaded at https://ladsweb.nascom.nasa.gov/. They were preprocessed with geometrical, radiometric, and atmospheric corrections and had Maximum Value Composites (MVC) to reduce the effects of clouds, atmosphere, and solar altitude angle (Fensholt and Proud, 2012). We used the MODIS Reprojection Tool (MRT) software to pre-process the data into TIF format, and the MVC method to generate monthly NDVI data products for semi-monthly data. Considering the influence of snowfall, the average annual NDVI value for the vegetation-growing season from April to October was selected for this study. These were calculated using data from September to October of the previous year and April–August of the current year. For example, the average NDVI values for 2014 were calculated using data from September 2013 to October 2013, and April to August 2014. Areas with average NDVI values less than 0.05 were defined as non-vegetated and were not included in the analysis.

### 2.2.3 LST data

The LST data were derived from MOD11A2 (h23v03, h23v04, h24v03, h24v04, h25v03, h25v04, h26v03, and h26v04) using with three land-level standard data products provided by NASA. Data were collected from September 2013 to August 2023 at a spatial resolution of 1000 m and a temporal resolution of eight days. Download from https://ladsweb.nascom.nasa.gov/. In this study, ENVI MODIS Conversion Toolkit (MCTK) was used to generate monthly LST data using the MVC method. The average LST for each year (April–October) was calculated using data from September and October of the previous year and data from April to August of the current year.

#### 2.2.4 Meteorological data

Air temperature and precipitation data were sourced from "Monthly Mean Temperature Data (1982–2021) at 1 km resolution on the Mongolian Plateau" and "Monthly Precipitation Data (1982–2021) at 1 km resolution on the Mongolian Plateau" from the National Science and Technology Infrastructure Platform (NSTIP) National Earth System Science Data Center (http://www.geodata.cn). The air temperature data were raw data read in format using the R language. The average air temperature data were downscaled using the delta downscaling scheme and validated using GSOD meteorological station data in ℃. The results were then output in TIF format. The raw precipitation data were read in NC format using R language, downscaled using the triangular downscaling scheme, and validated using GSOD meteorological station data in millimeters. The results were then output in the TIF format. In this study, monthly average air temperature and monthly precipitation data from September 2013 to August 2021 were selected and raster-processed using ArcMap10.6 software. Finally, the trends in the mean annual air temperature during the vegetation-growing season in the Mongolian Plateau permafrost region from 2014 to 2021 (Fig. 2) and the annual precipitation trends during the vegetation-growing season in the Mongolian Plateau permafrost region from 2014 to 2021 were obtained (Fig. 3).

### 2.3 Research methods

#### 2.3.1 Slope trend analysis

Trend analysis was applied to study the NDVI trend from September 2013 to August 2023 in the Mongolian Plateau permafrost region. The calculation formula is as follows (Stow et al., 2010):

$$slope = \frac{n\times\sum_{i=1}^{n}\left(i\times NDVI_i\right)-\sum_{i=1}^{n}i\times\sum_{i=1}^{n}NDVI_i}{n\sum_{i=1}^{n}i^2-\left(\sum_{i=1}^{n}i\right)^2} \quad (1)$$

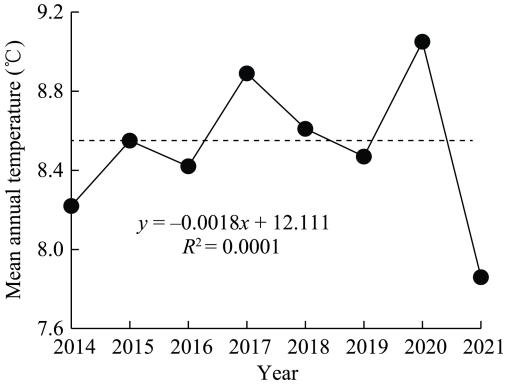


Fig. 2 Trends in mean annual air temperature during the vegetation growing season in the Mongolian Plateau permafrost region, 2014–2021

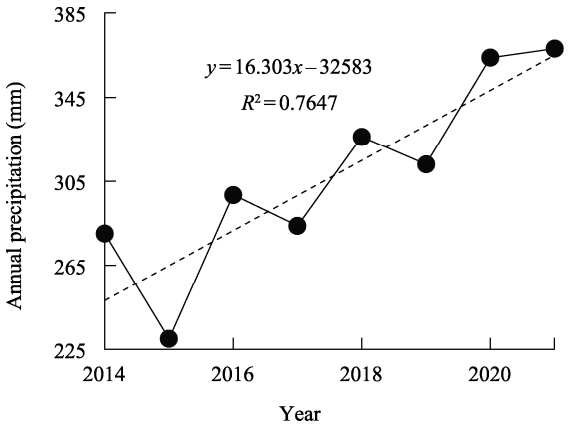


Fig. 3 Trends in annual precipitation during the vegetation growing season in the Mongolian Plateau permafrost region, 2014–2021

where, $slope$ is the slope of the NDVI trend from September 2013 to August 2023, $n$ is the number of years, and $NDVI_i$ is the average NDVI value for year $i$. A $slope>0$ indicates that the vegetation has an upward temporal trend. In contrast, a $slope<0$ indicates that vegetation has a downward temporal trend. The larger the absolute value of *slope*, the higher the rate of change.

#### 2.3.2 Mann-Kendall trend test

In this study, the Mann-Kendall (MK) trend test was used to test the significance of the annual mean NDVI for the vegetation growing season from 2014 to 2023. In the MK test, the original hypothesis H0 is that the time series data $(X_1, X_2, \cdots X_n)$ are $n$ independent, identically distributed samples of random variables. The alternative hypothesis H1 is a bilateral test that the distributions of $X_i$ and $X_j$ are not the same for $i, j \leqslant n$, with $i \neq j$. The statistic S for the test is calculated as follows (Yue and Wang, 2004):

$$S=\sum_{i=1}^{n-1}\sum_{j=i+1}^{n}sgn\left(X_j-X_i\right) \quad (2)$$

where $X_i$, $X_j$ are the observations corresponding to the *i*-th and *j*-th time series, respectively, and $i<j$, $sgn()$ is the sign function.

$$Sgn\left(X_j-X_i\right)=\begin{cases}1, & \left(X_j-X_i\right)>0\\ 0, & \left(X_j-X_i\right)=0\\ -1, & \left(X_j-X_i\right)<0\end{cases} \quad (3)$$

When $n\geqslant 8$, the statistic $S$ approximately follows a normal distribution with mean $E(S)=0$ and variance $Var(S)=n(n\text{-}1)(2n\text{+}5)/18$, irrespective of the presence of equivalent data points in the series. The standardized test statistic $Z$ was calculated as follows:

$$Z=\begin{cases}\dfrac{S-1}{\sqrt{Var(S)}} & S>0\\ 0 & S=0\\ \dfrac{S+1}{\sqrt{Var(S)}} & S>0\end{cases} \quad (4)$$

In the bilateral trend test, for a given confidence level (significance level) $\alpha$, if $|Z|\geqslant Z\left(1-\frac{\alpha}{2}\right)$, when the original hypothesis H0 is unacceptable, there is a significant upward or downward trend in the time-series data at the confidence level $\alpha$ (significance test level). A positive $Z$ value of $Z$ indicates an increasing trend, and a negative value indicates a decreasing trend. Absolute values of $Z$ greater than or equal to 1.645, 1.96, and 2.576 indicate that the test of significance was passed with confidence levels of 90%, 95%, and 99%, respectively.

#### 2.3.3 Correlation analysis

The spatial resolution of the NDVI data was set to 1000 m using the resampling method so that the spatial resolution of the other data was consistent. Image-by-image correlation analyses were conducted between the mean NDVI and LST for the vegetation-growing season in the Mongolian Plateau permafrost region annually from 2014 to 2023, and between the mean NDVI and air temperature (precipitation) for the vegetation-growing season in the permafrost region annually from 2014 to 2021 (Herrmann et al., 2005):

$$R_{xy}=\frac{\sum_{i=1}^{n}\left[(x_i-\bar{x})\times(y_i-\bar{y})\right]}{\sqrt{\sum_{i=1}^{n}(x_i-\bar{x})^2}\times\sqrt{\sum_{i=1}^{n}(y_i-\bar{y})^2}} \quad (5)$$

where $R_{xy}$ denotes the correlation coefficient of variables $x$ and $y$, with values between [−1, 1]; $x_i$ denotes the NDVI value for year $i$; $y_i$ denotes the LST (air temperature, precipitation) value for year $i$; $\bar{x}$ and $\bar{y}$ denote the mean values for NDVI and LST (air temperature, precipitation), respectively. $n$ is the number of years.

## 3 Results and analyses

### 3.1 Accuracy verification

To verify the accuracy of MODIS NDVI data, we obtained GIMMS and MOD13Q1 NDVI data from September 2013 to December 2015. We performed a correlation analysis between the monthly average NDVI of MOD13Q1 and GIMMS (Fig. 4). The NDVI values from the GIMMS data were generally lower than the NDVI values of the MODIS data. This was due to the lower spatial resolution of the GIMMS data at approximately 8 km. However, the two datasets showed a certain linear relationship, obtaining the equation $y$=1.2972$x$–0.3368 ($R$=0.9778), which passed the 0.001 significance level test. The long time series of monthly NDVI product data generated by MODIS with a spatial resolution of 250 m was found to be reliable and could be applied in this study.

### 3.2 NDVI trends during the vegetation growing season in the study area

#### 3.2.1 NDVI spatial distribution in the study area

The permafrost region of the Mongolian Plateau has a relatively high level of vegetation cover, with NDVI values increasing from southwest to northeast of the study area. As shown in Fig. 5, the area with vegetation $NDVI$>0.6 accounted for 52.8% of the entire study area, mainly in the northeast. The main vegetation cover type was forest, and some of the dominant vegetation was typical grassland and meadow grassland. The trees were mainly red pines, fir forests, and cedars (Wang et al., 2023). The area with NDVI values of 0.4–0.6 accounted for 26.9% of the study area. These values were mainly distributed in the central and eastern parts of the study area, with typical grasslands and desert steppes as the main vegetation cover types. A small proportion of the area was forested, with larch, cedar, birch, and aspen being the dominant tree taxa. The area has well-developed agriculture and animal husbandry and comprises a wide range of pastureland areas (Wang et al., 2023). The area with $NDVI$<0.4 are mainly located in the western and southern parts of the study area, accounting for 10.3% of the area. The main vegetation type was desert grassland,

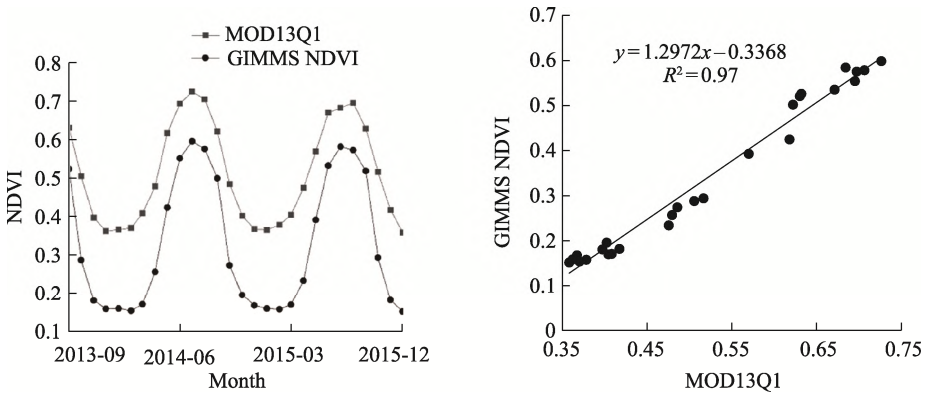


Fig. 4 Comparison of MOD13Q1 and GIMMS NDVI data

which has relatively little vegetation cover. It has been well-developed for animal husbandry and cultivation, mainly for cereals and potatoes (Wang et al., 2023). The NDVI values for the different types of permafrost regions had the following order: NDVI values of continuous and discontinuous permafrost regions > NDVI values of isolated or sparse permafrost regions > NDVI values of sporadic permafrost regions (Fig. 6).

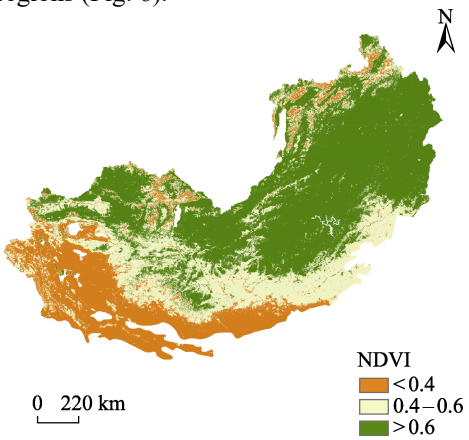


Fig. 5 Spatial distribution of average NDVI in vegetation growing season, 2014–2023

### 3.2.2 Characteristics of temporal and spatial changes of NDVI

As shown in Fig. 6, the average NDVI for the entire permafrost region and the three types of permafrost regions showed a decreasing trend during the growing season. The NDVI decreased from 0.6198 in 2014 to 0.5986 in 2023 for the entire permafrost region, with an average of 0.00212 per year. NDVI values varied between 0.67 and 0.71 for the continuous and discontinuous permafrost regions, between 0.48 and 0.56 for the isolated and sparse permafrost regions, and between 0.36 and 0.45 for the sporadic permafrost regions, with the highest NDVI stability in the continuous and discontinuous permafrost regions.

The MK (Mann-Kendall) test was used to derive the trend of NDVI changes in the permafrost region of the Mongolian Plateau (Fig. 7). A total of 59.4% of the study area showed a decreasing trend and 7.0% showed a significant decreasing trend ($P$<0.05). Areas with a significant decreasing trend were mainly in sporadic permafrost regions, where the dominant vegetation type is desert grasslands (Wang et al., 2023). There was an increasing trend in 40.6% of the areas, of which 5.4% showed a significant increasing trend ($P$<0.05). Areas with a significant increasing trend were mainly located in continuous permafrost regions. The main vegetation types are typical grasslands and forests (Wang et al., 2023). As shown in Table 1, the proportions of areas with an NDVI decreasing trend > 0.004 and the proportions of areas with an NDVI decreasing trend in the range of 0.002 to 0.004 in different types of permafrost regions are, in order, sporadic permafrost region > isolated and sparse permafrost region > continuous and discontinuous permafrost region. The proportion of the area with an

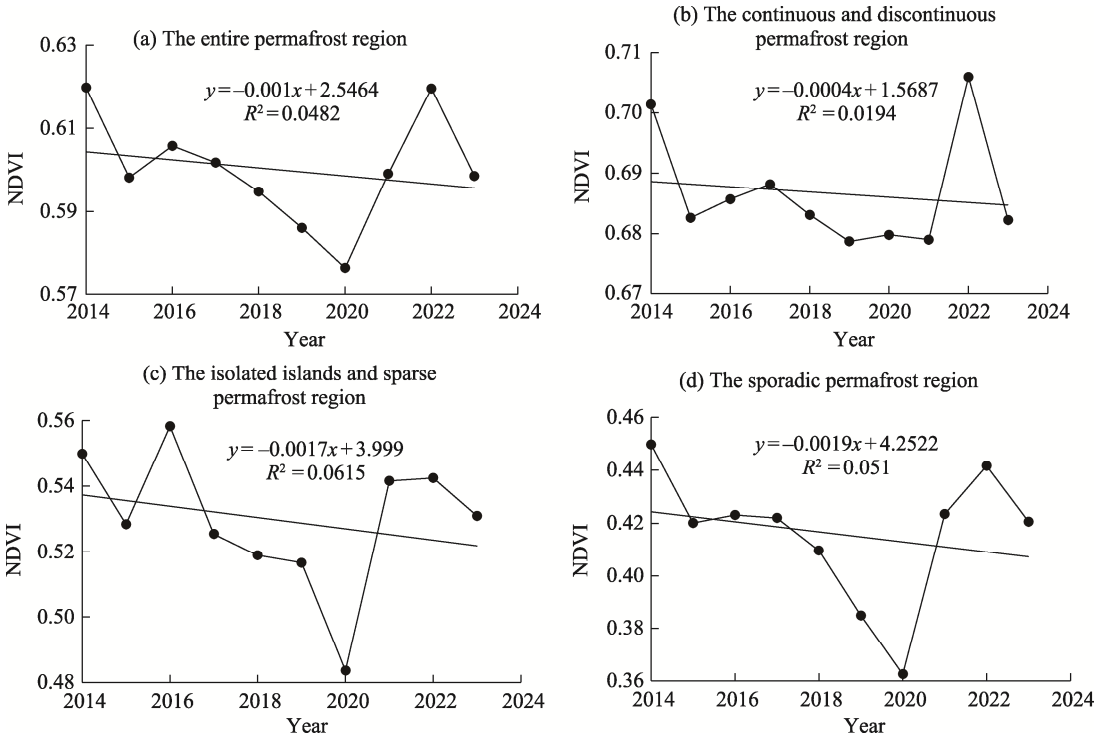


Fig. 6 Trends in annual mean NDVI during the vegetation growing season for different types of permafrost regions during the vegetation growing season, 2014–2023

Table 1 Proportion of area with NDVI trends in different types of permafrost regions during the vegetation growing season, 2014–2023

| Permafrost region types | NDVI trends (10 yr)$^{-1}$ | | | | | |
|---|---|---|---|---|---|---|
| | <–0.004 | –0.004– –0.002 | –0.002–0 | 0–0.002 | 0.002–0.004 | >0.004 |
| Continuous and discontinuous Permafrost region (%) | 19.8 | 14.9 | 18.2 | 16.1 | 11.8 | 19.2 |
| Isolated and sparse permafrost region (%) | 34.6 | 17.3 | 15.3 | 12.5 | 8.7 | 11.6 |
| Sporadic permafrost region (%) | 38.3 | 20.7 | 12.2 | 9.3 | 7.5 | 11.9 |
| Entire permafrost region (%) | 26.4 | 16.6 | 16.4 | 14.0 | 10.3 | 16.3 |

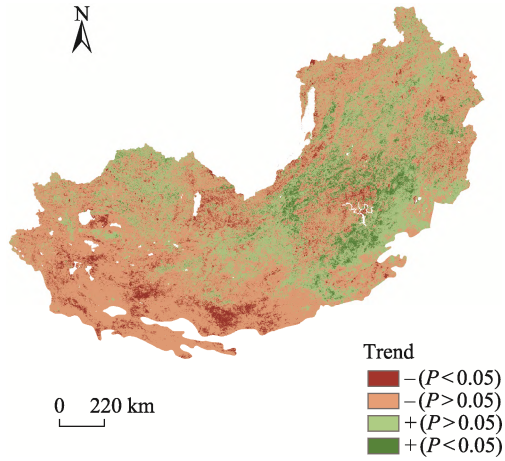


Fig. 7 Trends of average NDVI in vegetation growing season, 2014–2023

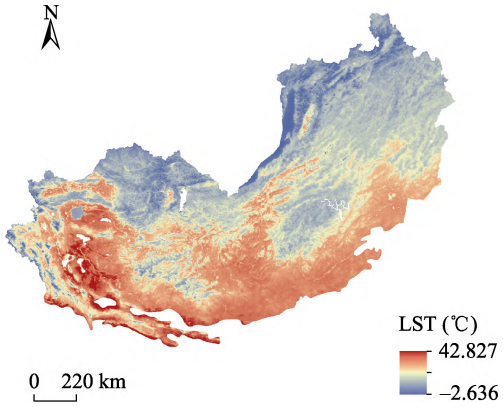


Fig. 8 Spatial distribution of the mean LST in the permafrost region of the Mongolian Plateau during the vegetation growing season, 2014–2023

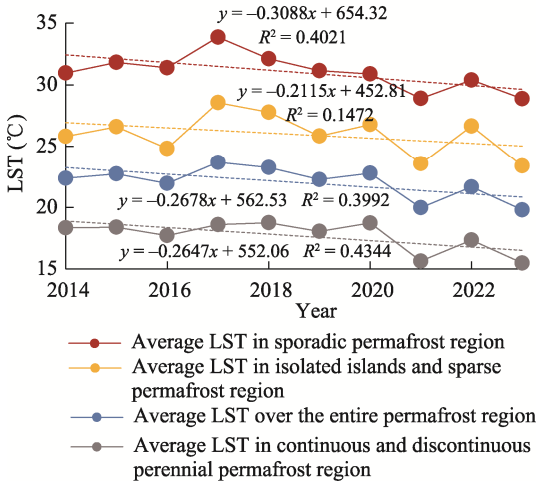


Fig. 9 Trends in average annual LST for the vegetation growing season in different types of permafrost regions, 2014–2023

increasing NDVI trend > 0.004 and the proportion of area with an increasing trend of 0.002 to 0.004 are, in order, continuous and discontinuous permafrost region > isolated and sparse permafrost region > sporadic permafrost region; The proportion of the area with a trend of −0.002 to 0.002 is in the order of continuous and discontinuous permafrost region > isolated and sparse permafrost region > sporadic permafrost region. The results showed that the most significant increase in NDVI was observed in the continuous and discontinuous permafrost regions. The most significant decreasing trend in NDVI was observed in sporadic permafrost regions. The most stable NDVI values were observed in continuous and discontinuous permafrost regions.

### 3.3 Correlation between NDVI and climate factors at the image metric scale

#### 3.3.1 Analysis of LST changes in the study area

As shown in Fig. 8, the average LST during the vegetation-growing season in the study area from 2014 to 2023 will gradually decrease from south to north. It also shows a correlation with the classification of permafrost regions. The annual mean LST of the vegetation growing season in different types of permafrost regions was in the following order: sporadic permafrost region > isolated and sparse permafrost region > continuous and discontinuous permafrost region, as shown in Fig. 9. The annual mean LST for different types of permafrost regions exhibited a decreasing trend, with the LST of continuous and discontinuous permafrost regions varying between 15.6 ℃ and 18.7 ℃. The LST of isolated and sparse permafrost regions varied between 23.4 ℃and 28.6 ℃, and the LST of sporadic permafrost regions varied between 28.8 ℃ and 33.9 ℃.

#### 3.3.2 Correlation between NDVI and LST

Correlation analyses of the annual mean NDVI and LST in different types of permafrost regions during the vegetation growing season from 2014 to 2023 showed a correlation

distribution between the NDVI and LST in different types of permafrost regions (Fig. 10a). The correlation coefficients for the entire permafrost region ranged from −0.992 to 0.989. The areas of non-significant negative correlation accounted for 41.3%, non-significant positive correlation accounted for 35.1%, significant negative correlation accounted for 17.0%, and significant positive correlation accounted for 6.6%. The correlation coefficients for continuous and discontinuous permafrost regions ranged from −0.992 to 0.985, with the largest area of 41.7% having a non-significant positive correlation, 36.5% having a non-significant negative correlation, 12.5% having a significant negative correlation and 9.3% having a significant positive correlation. The correlation coefficients for the isolated and sparse permafrost regions ranged from −0.900 to 0.963. Overall, 59.3% of the areas were not significantly negatively correlated, 25.9% were significantly negatively correlated, 13.9% were insignificantly positively correlated and 8.8% were significantly positively correlated. The correlation coefficients for the sporadic permafrost region ranged from −0.990 to 0.920; 42.9% of the area had a non-significant negative correlation, 34.5% had a non-significant positive correlation, 22.3% had a significant negative correlation and 0.3% had a significant positive correlation. The correlation coefficients were negative throughout most permafrost regions.

#### 3.3.3 Correlation between NDVI and air temperature

Correlation analysis of the annual mean NDVI values and annual mean air temperatures of different types of permafrost regions was conducted during the vegetation growing season from 2014 to 2021, and a distribution map for NDVI and air temperature correlation in the study area was obtained (Fig. 10b).

The percentage of negative correlation between NDVI and temperature in the different types of permafrost in the study area was larger than that of the positive correlation. The correlation coefficients of the entire permafrost area ranged from −0.996 to 0.996, with 57.4% of the area showing a non-significant negative correlation, 30.2% of the area showing a non-significant positive correlation, 8.5% of the area showing a significant negative correlation, and 3.8% of the area showing a significant positive correlation. The significant negative correlation areas were mainly distributed in the central isolated island and sparse permafrost areas of the study area. The correlation coefficients for the continuous and discontinuous permafrost regions ranged from −0.993 to 0.996, with the largest area of non-significant negative correlation accounting for 46.6% of the total area, non-significant positive correlation for 41.5% of the total area, significant negative correlation for 5.7% of the total area, and significant positive correlation for 6.2% of the total area. The correlation coefficients for the isolated and sparse permafrost areas ranged from −0.940 to 0.996. Among these, 73.0% of the areas were not significantly negatively correlated, 15.7% were significantly negatively correlated, 10.9% were not significantly positively correlated, and 0.4% were significantly positively correlated. The correlation coefficients for sporadic permafrost areas ranged from −0.928 to 0.992. 75.2% of the total area was not significantly negatively correlated, 13.9% was not significantly positively correlated, 10.9% was significantly negatively correlated, and 0.1% was significantly positively correlated.

#### 3.3.4 Correlation between NDVI and precipitation

Correlation analyses of the annual mean NDVI values and annual precipitation in different permafrost regions during the vegetation growing season from 2014 to 2021 were performed to obtain the distribution of correlation coefficients between NDVI and precipitation in the study area (Fig. 10c). The areas of positive correlation between NDVI and precipitation were greater than those of negative correlation in all types of permafrost, except for the continuous and discontinuous permafrost areas. The correlation coefficients ranged from −0.993 to 0.999 for the entire permafrost region, with 48.7% of the area having a non-significant positive correlation, 40.0% of the area having a non-significant negative correlation, 6.3% of the area having a significant positive correlation, and 5.0% of the area having a significant negative correlation. The correlation coefficients of the continuous and discontinuous permafrost region varied between −0.961 and 0.999, with the largest area of non-significant negative correlation accounting for 44.5% of the total area, a non-significant positive correlation for 42.1%, a significant positive correlation for 6.8%, and a significant negative correlation for 6.6%. The areas showing negative correlations in the continuous and discontinuous permafrost regions, such as Lake Baykal and Lake Hovsgol, were mostly located in the vicinity of the lake. In the isolated and sparse permafrost regions, 56.6% of the area showed no significant positive correlation, 36.3% showed no significant negative correlationed, 5.5% showed a significant positive correlation, and 1.5% showed a significant negative correlation. The isolated and sparse permafrost areas showing positive correlations were mainly distributed in the east, whereas areas with negative correlations were mainly distributed in the west. Sporadic permafrost areas showed 60.7% of non-significant positive correlations, 30.6% of non-significant negative correlations, 5.3% of significant positive correlations, and 3.3% of significant negative correlations. The sporadic permafrost region showing a positive correlation was mainly distributed in the east, the area of negative correlation was mainly distributed in the west, and the closer it was to the lakes (Uvs Nuur, Khara-Us-Nur and Kyrgyz), the more significant the negative correlation.

### 3.4 Correlation coefficients between NDVI and environmental factors

The correlation coefficients between the NDVI and environmental factors (LST, air temperature, and precipitation) were calculated. As shown in Table 2, in the entire permafrost

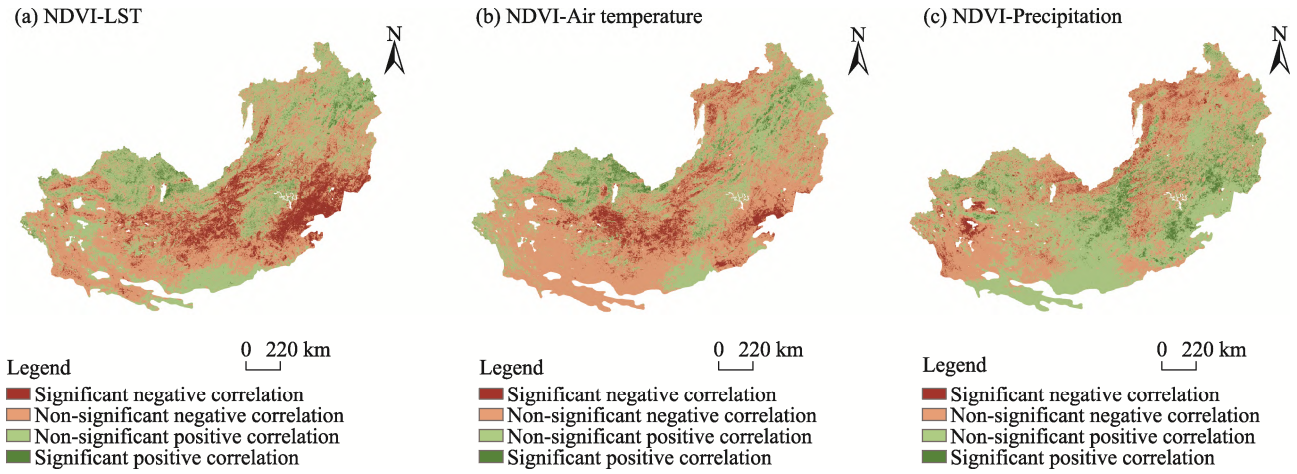


Fig. 10 Distribution of correlation coefficients between NDVI and environmental factors during the vegetation growing season in the Mongolian Plateau permafrost region

frost region, NDVI showed a non-significant negative correlation with LST ($r$=−0.139, $P$>0.5), NDVI showed a significant correlation with air temperature ($r$=−0.629, $P$<0.1), and NDVI showed a non-significant negative correlation with precipitation ($r$=−0.494, $P$<0.2). The main factors controlling the NDVI changes in the different types of permafrost regions were different. Air temperature had the most significant effect on the NDVI in the entire permafrost region, isolated and sparse permafrost regions, and sporadic permafrost regions. Precipitation had the most significant effect on the NDVI in the continuous and discontinuous permafrost regions. Overall, the correlation coefficients between the NDVI and air temperature in the Mongolian Plateau permafrost region were significantly higher for LST and precipitation.

Table 2 Correlation coefficients between mean NDVI and environmental factors during the vegetation growing season in different types of permafrost regions

| Permafrost type | Correlation coefficient | | |
|---|---|---|---|
| | LST | Air temperatures | Precipitation |
| Entire permafrost region | −0.139 | −0.629 | −0.494 |
| Continuous and discontinuous permafrost region | 0.128 | −0.145 | −0.498 |
| Isolated and sparse permafrost region | −0.397 | −0.736 | −0.117 |
| Sporadic permafrost region | −0.072 | −0.522 | −0.329 |

## 4 Discussion

### 4.1 NDVI trends

The degradation of alpine vegetation following permafrost degradation in a warming climate is a key research focus (Wang et al., 2008; Yang et al., 2012). Yang et al. (2010) showed that with further permafrost degradation, the soil moisture on the Tibetan Plateau decreased, and the soil environment became extremely arid. This has led to the disappearance of mesophytes in alpine meadows, the full expansion of drought-tolerant plants, and the gradual transformation of alpine meadows into alpine desert grasslands. Lara et al. (2016) showed that permafrost thawing in the boreal forests of the Alaskan lowlands increased as the climate warmed, with an estimated transition of approximately 15 km$^2$ or 7% of birch forests to wetlands and potentially drier vegetated ecosystems occurring between 1950 and 2009.

The Mongolian Plateau permafrost region is located in the transition zone between high-latitude and high-elevation permafrost regions, and has a specific regional effect. During the study period, there was a correlation between changes in vegetation cover and permafrost degradation. Sporadic permafrost areas showed the greatest decrease in vegetation, followed by isolated and sparse permafrost regions. The most significant increase in NDVI was in continuous and discontinuous permafrost, followed by isolated and sparse permafrost regions, and sporadic permafrost regions. The more stable the permafrost area, the more stable its vegetation cover in the context of environmental change. The environment for vegetation growth was optimized or maintained during the early stages of multi-year permafrost degradation. In highly degraded permafrost regions, where the soil contains less water and the ground temperature is higher, vegetation growth is unfavorable. Therefore, the degree of permafrost degradation increases and the trend of decreasing vegetation cover becomes more pronounced (Wang et al., 2006; Chen et al., 2010; Chen et al., 2011; Chen et al., 2012).

The NDVI in the different types of permafrost regions showed a decreasing trend during the vegetation growing season from 2014 to 2023. This was consistent with the results of an NDVI study conducted by Enebish in central Mongolia (Enebish et al., 2019). High levels of overgrazing and deforestation have been observed in the southern and central permafrost regions of the Mongolian Plateau (Shur

and Jorgenson, 2007; Klinge et al., 2021). These phenomena directly reduce vegetation cover and accelerate permafrost degradation. Therefore, further research is required to determine the strength of permafrost degradation on vegetation cover reduction.

### 4.2 NDVI correlation with environmental factors

#### 4.2.1 Correlation between NDVI and LST

Vegetation growth depends on appropriate hydrothermal conditions, and the relationship between NDVI and LST is commonly used to study hydrothermal constraints on vegetation growth (Kasischke and Turetsky, 2006; Xu et al., 2011; Yi et al., 2011; Piao et al., 2014; Zhou et al., 2015). In this study, continuous and discontinuous permafrost regions, isolated and sparse permafrost regions, and sporadic permafrost regions represented different stages of permafrost degradation. The continuous and discontinuous permafrost regions of the Mongolian Plateau had the largest areas of positive correlation between NDVI and LST, at approximately 51%, and the correlation coefficients showed a positive correlation. The NDVI-LST correlation was dominated by a negative correlation in isolated and sparse permafrost regions, and sporadic permafrost regions at with 85.2% and 56.79%, respectively. Wang et al. showed in their study on the NDVI-LST correlation on the Tibetan Plateau that the number of pixels with positive correlations was higher in cold regions, whereas the number of pixels with significant negative correlations was higher in the warm regions than in cold regions (Wang et al., 2016). This finding is consistent with the conclusions of this study. This conclusion suggests that, in the short term, the degradation of permafrost in regions where permafrost is well developed or maintained can promote vegetation growth and increase vegetation cover as LST increases, but the positive correlation between NDVI and LST during the vegetation growing season is weakened with further degradation of permafrost in the long term, the persistent increase in LST in permafrost regions can hinder vegetation growth (Guo et al., 2017b).

#### 4.2.2 Correlation between NDVI and air temperature

The vegetation growing season NDVI and air temperature had a non-significant negative correlation in the permafrost regions of the Mongolian Plateau during the vegetation growing season from 2014 to 2021. The negative correlation area ratios of isolated and sparse permafrost regions (88.7%), sporadic permafrost regions (86.1%), and continuous and discontinuous permafrost regions (52.3%) were similar to the correlation between NDVI and LST. Warmer air temperatures had the least negative effect on the NDVI in the continuous and discontinuous permafrost regions; nearly half (47.7%) of the continuous and discontinuous permafrost regions showed an increasing trend in vegetation cover with warmer air temperatures, whereas only 11.3% of the insular and sparse permafrost regions and 14% of the sporadic permafrost regions showed a trend of increasing vegetation cover. This is similar to the response of different types of permafrost distributions to changes in LST, where regions with well-maintained permafrost have more suitable environments for vegetation growth with increasing air temperatures, resulting in higher vegetation cover. As permafrost degrades, rising air temperature deteriorate the environment in which vegetation grows, thereby reducing vegetation cover.

#### 4.2.3 Correlation between NDVI and precipitation

NDVI and precipitation had a non-significant positive correlation in most areas of the Mongolian Plateau permafrost region during the vegetation growing season from 2014 to 2021. The proportion of negatively correlated areas (51.1%) was larger than that of positively correlated areas in the continuous and discontinuous permafrost regions. The proportion of positively correlated areas in isolated and sparse permafrost regions was 62.1%, where the proportion of positively correlated areas in sporadic permafrost regions was 66.0%. Representing the process of permafrost degradation in different types of permafrost regions, in regions where permafrost is well maintained, increased precipitation hinders vegetation growth because of high soil water content. As permafrost degradation increases, the soil water content becomes insufficient for vegetation growth, and increased precipitation favors vegetation growth. In the area around a lake, the closer it is to the lake, the more water is provided to the surrounding area. The soil environment is sufficient for vegetation growth, whereas an increase in precipitation is counterproductive to vegetation growth.

## 5 Conclusions

To address the recent influence of climate change on vegetation in permafrost areas, we investigated the spatial and temporal NDVI trends in the Mongolian Plateau permafrost region during the vegetation growing season. The correlation between NDVI and the environmental factors of different types of permafrost regions was analyzed, and the following conclusions were drawn:

(1) The average NDVI in the permafrost region of the Mongolian Plateau showed a non-significant decreasing trend during the 2014–2023 vegetation growing season, with an average annual decrease of 0.00212. Different permafrost degradation stages have different effects on the NDVI. Continuous and discontinuous permafrost regions had the largest percentages of areas with increasing NDVI values. The sporadic permafrost regions had the largest percentage of area with decreasing NDVI values.

(2) The average NDVI during the vegetation growing season throughout the permafrost region was negatively correlated with LST, air temperature, and precipitation. The most significant correlation was between the NDVI and air temperature. The main factors controlling NDVI changes in the different types of permafrost regions were different. Air temperature had the most significant effect on the NDVI in

the isolated, sparse, and sporadic permafrost regions. Precipitation had the most significant effect on the NDVI in the continuous and discontinuous permafrost regions.

This study has some limitations. Only the effects of air temperature, precipitation, and LST on NDVI were considered; other factors may also have important effects on vegetation growth in the study area. For example: 1) The effects of soil moisture, soil temperature, and other factors on the NDVI in the Mongolian Plateau permafrost region have not yet been considered. The roles of other environmental factors in this region should be strengthened in the future. 2) Different soil textures affect vegetation differently, and the amount of gravel has a significant effect on grassland plant growth (Qin et al., 2015). Therefore, it is important to study the effects of different soil texture characteristics on the vegetation. 3) The direct and indirect effects of anthropogenic disturbances such as overgrazing on permafrost vegetation have not been studied. The gnawing and trampling of vegetation directly contribute to a reduction in vegetation cover. Reduced vegetation cover leads to the retention of water, radiation, and evapotranspiration by the vegetation canopy and affects LST and soil moisture content (Yi et al., 2013; Wang et al., 2016).

In the future, we will continue to investigate the long-term series response of NDVI to climate change in the permafrost region of the Mongolian Plateau. In addition, it extends to large permafrost areas in Northern Asia and other regions.

## References


Baltzer J L, Veness T, Chasmer L E, et al. 2014. Forests on thawing permafrost: Fragmentation, edge effects, and net forest loss. *Global Change Biology*, 20(3): 824–834.

Beilman D W. 2001. Plant community and diversity change due to localized permafrost dynamics in bogs of western Canada. *Canadian Journal of Botany*, 79(8): 983–993.

Bhatt U, Walker D, Raynolds M, et al. 2013. Recent declines in warming and vegetation greening trends over Pan-Arctic Tundra. *Remote Sensing*, 5(9): 4229–4254.

Chen S Y, Liu W J, Qin X, et al. 2012. Response characteristics of vegetation and soil environment to permafrost degradation in the upstream regions of the Shule River Basin. *Environmental Research Letters*, 7(4): 045406. DOI: 10.1088/1748-9326/7/4/045406.

Chen S Y, Liu W J, Ye B S, et al. 2011. Species diversity of the vegetation in relation to biomass and environmental factors in the upper area of Shule River. *Acta Prataculturae Sinica*, 20(3): 70–83. (in Chinese)

Chen S Y, Zhao L Z, Qin D H, et al. 2010. A preliminary study on relationships between alpine grassland biomass and environmental factors in the permafrost regions of Qinghai-Tibet Plateau. *Journal of Glaciology and Geocryology*, 32(2): 405–413. (in Chinese)

Enebish B, Dashkhuu D, Renchin M, et al. 2019. Impact of climate on the NDVI of Northern Mongolia. *Journal of the Indian Society of Remote Sensing*, 48(2): 333–340.

Fensholt R, Proud S R. 2012. Evaluation of Earth observation based global long term vegetation trends—Comparing GIMMS and MODIS global NDVI time series. *Remote Sensing of Environment*, 119: 131–147.

Gao H D, Sa C L, Meng F H, et al. 2022. Temporal and spatial characteristics of permafrost on Mongolian Plateau from 2003 to 2009. *Journal of Arid Land Resources and Environment*, 36(3): 99–106. (in Chinese)

Gao W F. 2019. Emission characteristics and influencing factors of greenhouse gas in the continuous permafrost region of Daxing'an Mountains, Northeast China. Diss., Harbin, China: Northeast Forestry University. (in Chinese)

Guo J T, Hu Y M, Bu R C. 2022. Effect of degradation of permafrost in the northeast of China on seasonal change of vegetation NDVI. *Journal of Inner Mongolia Normal University* (*Natural Science Edition*), 51(1): 50–56. (in Chinese)

Guo J T, Hu Y M, Xiong Z P, et al. 2017a. Variations in growing-season NDVI and its response to permafrost degradation in Northeast China. *Sustainability*, 9(4): 511. DOI: 10.3390/su9040551.

Guo J T, Hu Y M, Xiong Z P, et al. 2017b. Spatiotemporal variations of growing-season NDVI and response to climate change in permafrost zone of Northeast China. *Chinese Journal of Applied Ecology*, 28(8): 2413–2422. (in Chinese)

Herrmann S M, Anyamba A, Tucker C J. 2005. Recent trends in vegetation dynamics in the African Sahel and their relationship to climate. *Global Environmental Change*, 15(4): 394–404.

Jorgenson M T, Racine C H, Walters J C, et al. 2001. Permafrost degradation and ecological changes associated with a warming climate in Central Alaska. *Climatic Change*, 48(4): 551–579.

Kasischke E S, Turetsky M R. 2006. Recent changes in the fire regime across the North American boreal region—Spatial and temporal patterns of burning across Canada and Alaska. *Geophysical Research Letters*, 33(9): 703. DOI: 10.1029/2006GL025677.

Klinge M, Schneider F, Dulamsuren C, et al. 2021. Interrelations between relief, vegetation, disturbances, and permafrost in the forest—steppe of Central Mongolia. *Earth Surface Processes and Landforms*, 46(9): 1766–1782.

Lara M J, Genet H, McGuire A D, et al. 2016. Thermokarst rates intensify due to climate change and forest fragmentation in an Alaskan boreal forest lowland. *Global Change Biology*, 22(2): 816–829.

Li X. 2019. The Russian frozen soil dataset (1:250000). National Cryosphere Desert Data Center (www.ncdc.ac.cn). DOI: 10.12072/ncdc.westdc.db3802.

Liu S, Yu G R, Qian Z S, et al. 2009. The thawing-freezing processes and soil moisture distrubution of the steppe in central Mongolian Plateau. *Acta Pedologica Sinica*, 46(1): 46–51. (in Chinese)

Ma X, Wu T H, Zhu X F, et al. 2022. Spatiotemporal variations in the air freezing and Thawing Index over the Mongolian Plateau from 1901 to 2019. *Frontiers in Environmental Science*, 10. DOI: 10.3389/fenvs.2022.875450.

Mao D H, Luo L, Wang Z M, et al. 2015. Variations in net primary productivity and its relationships with warming climate in the permafrost zone of the Tibetan Plateau. *Journal of Geographical Sciences*, 25(8): 967–977.

Piao S L, Nan H J, Huntingford C, et al. 2014. Evidence for a weakening relationship between interannual temperature variability and northern vegetation activity. *Nature Communications*, 5: 6018. DOI: 10.1038/ncomms6018.

Qin Y, Yi S H, Chen J J, et al. 2015. Effects of gravel on soil and vegetation properties of alpine grassland on the Qinghai-Tibetan Plateau. *Ecological Engineering*, 74: 351–355.

Qin Y, Yi S, Ren S, et al. 2013. Responses of typical grasslands in a semi-arid basin on the Qinghai-Tibetan Plateau to climate change and disturbances. *Environmental Earth Sciences*, 71(3): 1421–1431.

Schuur E A G, Crummer K G, Vogel J G, et al. 2007. Plant species composition and productivity following permafrost thaw and thermokarst in Alaskan Tundra. *Ecosystems*, 10(2): 280–292.

Short N, Brisco B, Couture N, et al. 2011. A comparison of TerraSAR-X, RADARSAT-2 and ALOS-PALSAR interferometry for monitoring permafrost environments: Case study from Herschel Island, Canada. *Remote Sensing of Environment*, 115(12): 3491–3506.

Shur Y L, Jorgenson M T. 2007. Patterns of permafrost formation and degradation in relation to climate and ecosystems. *Permafrost and Periglacial Processes*, 18(1): 7–19.

Sodnom N, Yanshin A L. 1990. Map of permafrost and permafrost zoning in the Republic of Mongolia. National Cryosphere Desert Data Center (www.ncdc.ac.cn). DOI: 10.12072/ncdc.westdc.db3667.2023.

Stow D, Daeschner S, Hope A, et al. 2010. Variability of the Seasonally Integrated Normalized Difference Vegetation Index across the north slope of Alaska in the 1990s. *International Journal of Remote Sensing*, 24(5): 1111–1117.

Strozzi T, Antonova S, Günther F, et al. 2018. Sentinel-1 SAR interferometry for surface deformation monitoring in low-land permafrost areas. *Remote Sensing*, 10(9): 1360. DOI: 10.3390/rs10091360.

Sun Z G, Wang Q X, Xiao Q A, et al. 2014. Diverse responses of remotely sensed grassland Phenology to interannual climate variability over frozen ground regions in Mongolia. *Remote Sensing*, 7(1): 360–377.

Tutubalina O V, Rees W G. 2001. Vegetation degradation in a permafrost region as seen from space: Noril'sk (1961–1999). *Cold Regions Science and Technology*, 32(2–3): 191–203.

Vrieling A, Leeuw J D, Said M Y. 2013. Length of growing period over Africa: Variability and trends from 30 years of NDVI time series. *Remote Sensing*, 5(2): 982–1000.

Wang C, Zhang Z J, Zhang H, et al. 2018. Active layer thickness retrieval of Qinghai-Tibet permafrost using the TerraSAR-X InSAR technique. *IEEE Journal of Selected Topics in Applied Earth Observations and Remote Sensing*, 11(11): 4403–4413.

Wang G X, Li Y S, Wang Y B, et al. 2008. Effects of permafrost thawing on vegetation and soil carbon pool losses on the Qinghai-Tibet Plateau, China. *Geoderma*, 143(1–2): 143–152.

Wang G X, Li Y S, Wu Q B, et al. 2006. Impacts of permafrost changes on alpine ecosystem in Qinghai-Tibet Plateau. *Science in China Series D*: *Earth Sciences*, 49(11): 1156–1169.

Wang J L, Xu S X, Yang F, et al. 2023. A dataset of land cover classifications with a spatial resolution of 30 m in Mongolia in 2005 and 2015. *China Scientific Data*, 8(1): 8–20. (in Chinese)

Wang S P, Duan J C, Xu G P, et al. 2012. Effects of warming and grazing on soil N availability, species composition, and ANPP in an alpine meadow. *Ecology*, 93(11): 2365–2376.

Wang X Y, Yi S H, Wu Q B, et al. 2016. The role of permafrost and soil water in distribution of alpine grassland and its NDVI dynamics on the Qinghai-Tibetan Plateau. *Global and Planetary Change*, 147: 40–53.

Xu W X, Gu S, Zhao X Q, et al. 2011. High positive correlation between soil temperature and NDVI from 1982 to 2006 in alpine meadow of the Three-River Source Region on the Qinghai-Tibetan Plateau. *International Journal of Applied Earth Observation and Geoinformation*, 13(4): 528–535.

Yang Z P, Gao J X, Zhao L, et al. 2012. Linking thaw depth with soil moisture and plant community composition: effects of permafrost degradation on alpine ecosystems on the Qinghai-Tibet Plateau. *Plant and Soil*, 367(1–2): 687–700.

Yang Z P, Ouyang H, Xu X L, et al. 2010. Effects of permafrost degradation on ecosystems. *Acta Ecologica Sinica*, 30(1): 33–39. (in Chinese)

Yi S, Li N, Xiang B, et al. 2013. Representing the effects of alpine grassland vegetation cover on the simulation of soil thermal dynamics by ecosystem models applied to the Qinghai-Tibetan Plateau. *Journal of Geophysical Research*: *Biogeosciences*, 118(3): 1186–1199.

Yi S H, Zhou Z Y, Ren S L, et al. 2011. Effects of permafrost degradation on alpine grassland in a semi-arid basin on the Qinghai-Tibetan Plateau. *Environmental Research Letters*, 6(4): 5403. DOI: 10.1088/1748-9326/6/4/ 045403.

Yue S, Wang C Y. 2004. The Mann-Kendall test modified by effective sample size to detect trend in serially correlated hydrological series. *Water Resources Management*, 18(3): 201–218.

Zhang T, Heginbottom J A, Barry R G, et al. 2000. Further statistics on the distribution of permafrost and ground ice in the Northern Hemisphere. *Polar Geography*, 24(2): 126–131.

Zhou X Y, Shi H D, Wang X R, et al. 2012. Analysis of spatiotemporal characteristics and drivers of land use changes in the Mongolian Plateau over the past 30 years. *Acta Agriculturae Zhejiangensis*, 24(6): 1102–1110. (in Chinese)

Zhou Z Y, Yi S H, Chen J J, et al. 2015. Responses of alpine grassland to climate warming and permafrost thawing in two basins with different precipitation regimes on the Qinghai-Tibetan Plateau. *Arctic Antarctic and Alpine Research*, 47(1): 125–131.

# 蒙古高原多年冻土区 2014–2023 年植被变化及其对气候变化的响应

李凤娇[1,2]，王卷乐[2,3,4]，李朋飞[1]，Davaadorj DAVAASUREN[5]

1. 西安科技大学测绘科学与技术学院，西安 710054；
2. 中国科学院地理科学与资源研究所资源与环境信息系统国家重点实验室，北京 100101；
3. 中国科学院大学资源与环境学院，北京 100049；
4. 江苏省地理信息资源开发与应用协同创新中心，南京 210023;
5. 蒙古国立大学艺术与科学学院地理系，乌兰巴托 14201, 蒙古

**摘　要：**多年冻土区是对气候变化最敏感的地区之一。随着全球变暖，蒙古高原多年冻土退化加剧，多年冻土区植被生态系统受到严重威胁。面对这一挑战，了解气候变化下蒙古高原不同冻土退化阶段的植被变化至关重要。本文基于多年冻土分布图，依据“空间代替时间”的理念，划分了不同的多年冻土带，探讨了 2014–2023 年多年冻土退化不同阶段植被对气候变化的响应。研究结果表明：（1）研究区 NDVI 值呈下降趋势，下降所占面积比例依次为零星多年冻土区>孤岛和稀疏多年冻土区>连续和不连续多年冻土区。（2）不同类型多年冻土区植被生长的主控因子不同，气温是孤岛和稀疏多年冻土区（$r$=–0.736）以及零星多年冻土区（$r$=–0.522）植被生长的主控因子，降水是连续和不连续多年冻土区（$r$=–0.498）植被生长的主控因子。（3）在不同的多年冻土退化阶段，NDVI 对气候变化的响应各不相同。在多年冻土退化初期，地表温度和气温升高有利于植被生长，增加植被覆盖，降水量的增加则会阻碍植被生长；随着多年冻土退化，地表温度和气温升高会阻碍植被生长，降水量的增加则会促进植被生长。

**关键词：**蒙古高原；MODIS；NDVI；多年冻土；植被退化